



Personal authentication using palm-print features [☆]

Chin-Chuan Han^{a, *}, Hsu-Liang Cheng^b, Chih-Lung Lin^b, Kuo-Chin Fan^b

^aDepartment of Computer Science and Information Engineering, Chung-Hua University, 30 Tung Shiang, Hsinchu 300, Taiwan, Republic of China

^bDepartment of Computer Science and Information Engineering, National Central University, Chungli, Taiwan, Republic of China

Received 21 December 2001

Abstract

Biometrics-based authentication is a verification approach using the biological features inherent in each individual. They are processed based on the identical, portable, and arduous duplicate characteristics. In this paper, we propose a scanner-based personal authentication system by using the palm-print features. It is very suitable in many network-based applications. The authentication system consists of enrollment and verification stages. In the enrollment stage, the training samples are collected and processed by the *pre-processing*, *feature extraction*, and *modeling* modules to generate the matching templates. In the verification stage, a query sample is also processed by the pre-processing and feature extraction modules, and then is matched with the reference templates to decide whether it is a genuine sample or not. The region of interest (ROI) for each sample is first obtained from the pre-processing module. Then, the palm-print features are extracted from the ROI by using Sobel and morphological operations. The reference templates for a specific user are generated in the modeling module. Last, we use the template-matching and the backpropagation neural network to measure the similarity in the verification stage. Experimental results verify the validity of our proposed approaches in personal authentication. © 2002 Pattern Recognition Society. Published by Elsevier Science Ltd. All rights reserved.

Keywords: Personal authentication; Palmprint features; Multi-template matching; Backpropagation neural network

1. Introduction

Recently, biometric features have been widely used in many personal authentication applications because they possess the following physiological properties [1]: *universality*, *uniqueness*, *permanence*, *collectability*, *performance*, *acceptability*, and *circumvention*. According to the above properties, many access control systems adopt biometric features to replace the digit-based password. Biometric features are the features extracted from human biological organs or behavior. The first book addressing various biometric technologies for personal identification in networked society was edited by Jain et al. in 1999 [2]. In this book, they make

a detail comparison of 14 different biometric technologies. O’Gorman [3] also surveyed six biometric features in matching, validation, maximum independent samples per person, sensor cost, and sensor-size topics. Though fingerprint and eye features provide a very high recognition rate, they are unsuitable for identification systems. First, the sensor cost of eye-based features is too high to implement in many low security demanding applications such as computer, home security systems, restricted entry control, corporate networks, etc. Besides, since fingerprint features are used officially in criminal investigations and commercial transactions, most of the users are unwilling to deliver their fingerprint data to a company or system for privacy reason. Jain et al. [2] mentioned that “The match between a biometrics and an application is determined depending upon the requirements of the given application, the characteristics of the applications and properties of the biometrics.” In this paper, we propose a palm-print-based technology to identify the individuals in the entry control systems.

[☆] This work is supported by National Science Council of Taiwan under Grant No. NSC89-2213-E-343-004.

* Corresponding author. Tel.: +886-3-5374281x8306; fax: +886-3-5374281.

E-mail address: cchan@chu.edu.tw (C.-C. Han).

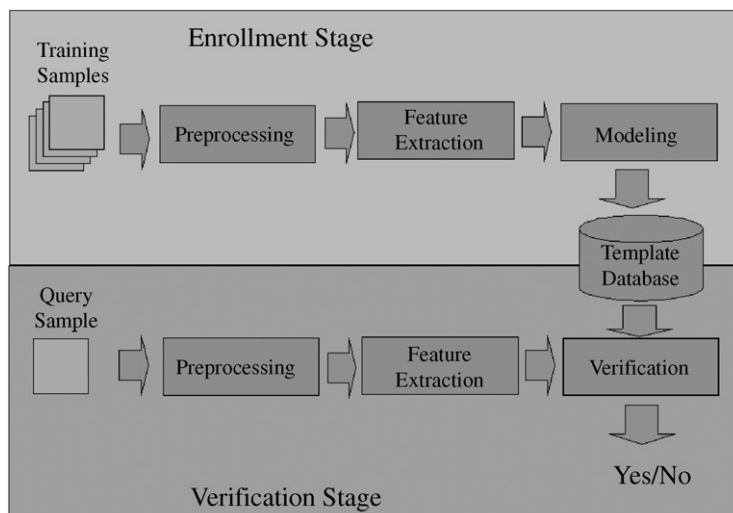


Fig. 1. The modules of biometric-based verification systems.

Golfarelli et al. [4] extracted 17 hand shape features to verify the personal identity. Zunkel [5] introduced a commercial product of hand-geometry-based recognition and applied it to many access control systems. Jain et al. [6] used the deformable matching techniques to verify the individuals via the hand shapes. The hand-shape of test sample is aligned with that in the database, and a defined distance is calculated for the evaluation of similarity. 96.5% accuracy rate and 2% false acceptance rate (FAR) are achieved in their approaches. Zhang and Shu [7] applied the datum point invariant property and the line feature matching technique to conduct the verification process via the palm-print features. They inked the palm-print on the papers and then scanned them to obtain 400×400 images. It is not suitable for many on-line security systems because two steps are needed to obtain the palm-print images in their approach. Kung et al. [8] designed a decision-based neural network (DBNN) classifier and applied it to face recognition and the palm-print verification. Joshi et al. [9] captured an image of middle finger by using a CCD camera to generate the wide line integrated profile (WLIP) of length 472. They also used the normalized correlation function to compute the similarity values between the input sample and the reference templates. Furthermore, Zhang [10] proposed a texture-based feature extraction method to obtain the global attributes of a palm. Besides, a dynamic selection scheme was also designed to ensure the palm-print samples to be correctly and effectively classified in a large database.

In many lectures, two possible biometric features can be extracted from human hands. First, hand-shape geometrical features such as finger width, length, and thickness are the well-known features adopted in many systems. These features frequently vary due to the wearing of rings in fingers. Besides, the width or thickness of women's fingers will

rapidly vary in a short time due to the pregnancy. According to the variation of hand geometry, it can be used in the entry control systems with low security requirements and a low rejection rate to record the entry data of employees or users. Besides, the reference features in the database should be updated frequently. Comparing with the palm shape features, the relatively stable feature extracted from the hands is the print of palms. In this paper, we utilize the palm-print features to do the matching process.

In addition to the feature selection, the capturing device is another important performance index to be evaluated in the biometrics-based verification systems. In many hand-shape-based capturing devices, users have to put their hands on a panel with some fixed pegs to avoid the rotation and translation problems. This mechanism makes some users feel uncomfortable. Furthermore, the capturing devices using the CCD camera provide poor quality images. The light factor will deeply affect the image quality and the resolution of CCD camera is not sufficiently high to obtain the high-quality images. To resolve the above problems, we adopt an optical scanner to serve as the acquiring device in our work.

In this paper, we propose a scanner-based personal authentication system by using the palm-print features. Two stages, *enrollment* and *verification*, constitute the identification system as shown in Fig. 1. In the enrollment stage, M hand images of an individual are collected as the training samples. These samples should be processed by the *pre-processing*, *feature extraction*, and *modeling* modules to generate the matching templates. In the verification stage, a query sample is also processed by the pre-processing and feature extraction modules, and is then matched with the templates to decide whether it is a genuine sample or not. In our proposed palm-print-based identification system,

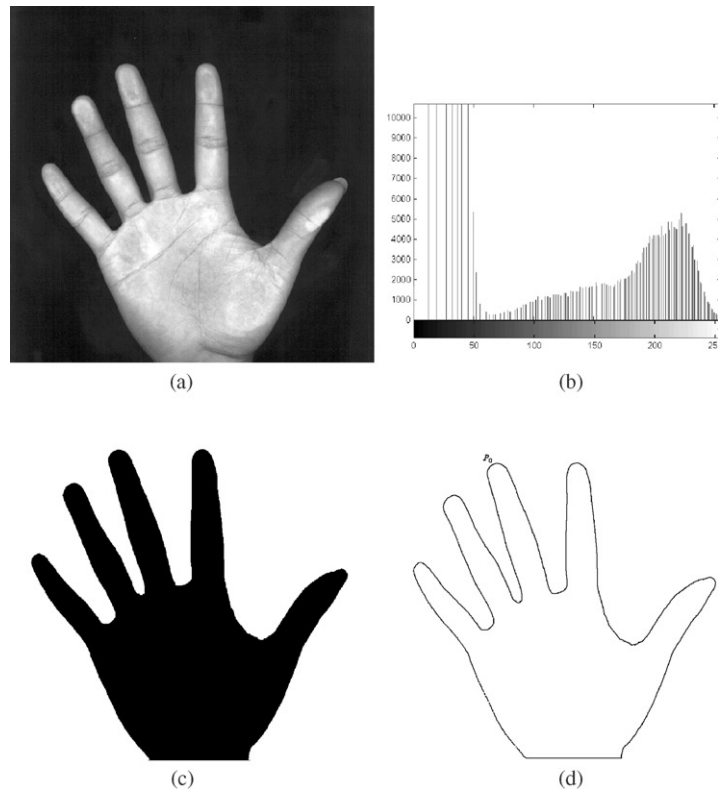


Fig. 2. The image-thresholding and border-tracing: (a) a hand image scanned in 100 dpi resolution; (b) the histogram diagram of (a); (c) the binary image; (d) the contour of hand shape.

the pre-processing module, including *image thresholding*, *board tracing*, *wavelet-based segmentation*, and *ROI location* steps, should be performed to obtain a square region in a palm table which is called region of interest (ROI). Then, we perform the feature extraction process to obtain the feature vectors by the Sobel and morphological operations. The reference templates for a specific user are generated in the modeling module. In the verification stage, we use the template matching and backpropagation neural network to measure the similarity between the reference templates and test samples.

The rest of this paper is organized as follows. In Section 2, four steps for the pre-processing module are executed to find the location of ROI. The feature extraction techniques, including Sobel's and morphological operations are described in Section 3. The modeling procedure for the verification purpose is introduced in Section 4. First, the simple and practical multiple template matching method is designed in the section to evaluate the similarity between the query and reference samples. The BP-based NN is also built in Section 4 to compute the similarity values for verification. In Section 5, experimental results are demonstrated to verify the validity of our proposed algorithms. Finally, some concluding remarks are given in Section 6.

2. Preprocessing

Image preprocessing is usually the first and essential step in pattern recognition. In our proposed approach, four steps are devised in the pre-processing module. Image thresholding, border tracing, wavelet-based segmentation, and ROI location are sequentially executed to obtain a square region which possesses the palm-print data. In the following contexts, we will present the details of each step.

Step 1: Image thresholding. The hand images of 256 gray levels are acquired from a platform scanner as shown in Fig. 2(a). The image-thresholding operation is to binarize the gray images to obtain the binary hand-shape images. In this step, the histogram of gray images are analyzed as shown in Fig. 2(b) to determine a threshold value. This value is automatically set at the local minimal value between 50 and 100. Since the capturing environment is stable and controlled, the threshold value is conveniently fixed to be 70 in our experiments. Thus, the binarized image can be obtained as shown in Fig. 2(c).

Step 2: Border tracing. After the image-thresholding step, the binary images are traced to obtain the contours of hand shape by making use of the border tracing algorithm. The

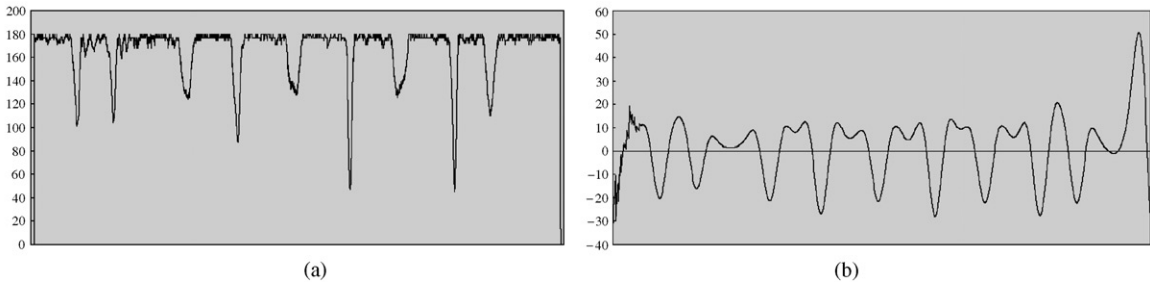


Fig. 3. (a) The profile of curvature of hand shape; (b) the transformed profile of high-frequency sub-band.

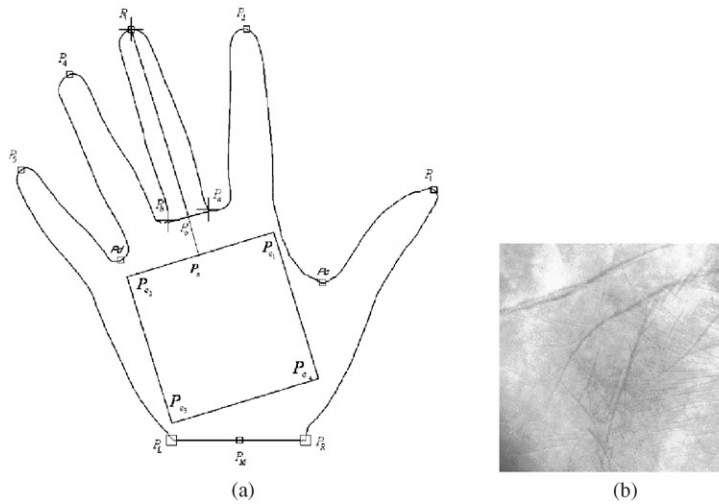


Fig. 4. The generation of region of interest (ROI).

main purpose of this step is to find the boundary of a hand image and then locate the positions of five fingers for the determination of palm table. A square region in the palm table called ROI will be generated. At the beginning, the first point of hand shape is set at the upper-left point of a hand-shape image. The contour of hand shape is then traced in counter-clockwise direction. In our experiments, eight neighborhood directions are adopted in the border tracing algorithm. The coordinates of each traced pixel should be maintained to represent the shape of the hand. The traced contours of the hand image in Fig. 2(a) are shown in Fig. 2(d). The details of border tracing algorithm can be found in Ref. [11].

Step 3: Wavelet-based segmentation. In the previous step, the border pixels of hand shape are sequentially traced and represented by a set of coordinates $(x_i, y_i), i = 1, 2, \dots$. In this step, the wavelet-based segmentation technique is adopted to find the locations of five finger tips and four finger roots. As is known, these points are located at the corner of hand shape. According to the definition for corner, the corners should be located at the points with a high curvature or at the points whose curvature is local minimal. First,

the set of coordinates is transformed into the profile of curvature as depicted in Fig. 3(a). The profile of curvature is then transformed to multi-resolucional signals of low- and high-frequency sub-bands. Since the crucial points $P_a, P_b,$ and P_3 of corner points (see Fig. 4(a)) determine the ROI location in the palm table, it is very important to explicitly locate the corner points of hand-shape. The wavelet transform can provide stable and effective segmented results in corner detection. Here, the transformed signals of high-frequency sub-band are depicted in Fig. 3(b). From these signals, the corners are labeled at the local minimal points of negative magnitude which can be located between two zero-crossing points. The detected corner points in Fig. 2(d) are illustrated in Fig. 4(a).

Step 4: ROI generation. In this step, we will find the region of interest (abbreviated as ROI) in the palm table as shown in Fig. 4 which is the operating region both in the enrollment and verification processes. In acquiring the hand-images, the hands were freely put on the plate-form scanner at any position and in any direction. Fortunately, when users put their hand on the input devices in normal

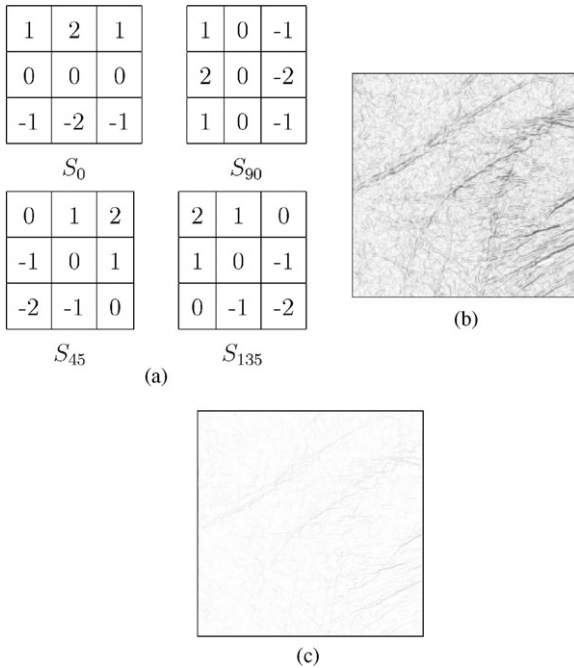


Fig. 5. (a) Four Sobel operators; (b) the features operated via Sobel operation; (c) the features operated via morphological operation.

condition, the direction of a hand is consistent with the principal axis which is the center line of middle finger. According to the result generated in Step 3, the location of ROI is determined from points P_a, P_b, P_3 , and the geometrical formula. Two points P_a and P_b are the base points to generate the ROI. First, the middle point P_0 is calculated from points P_a and P_b . Then, the principal axis $\overline{P_0P_3}$ is obtained which is the center line of middle finger perpendicular to line $\overline{P_aP_b}$. The principal axis $\overline{P_0P_3}$ is then extended to point P_e , where $|\overline{P_0P_e}| = |\overline{P_aP_b}|$. From point P_e , the two perpendicular bisector lines denoted as $\overline{P_eP_{e_2}}$ and $\overline{P_eP_{e_1}}$, whose length equals 128 pixels, are found. Based on this section line $P_{e_1}P_{e_2}$, the square region $P_{e_1}P_{e_2}P_{e_3}P_{e_4}$ of size 256 by 256 is defined as the ROI, as shown in Fig. 4(a). From these four points, the image of ROI is cut from the hand image as shown in Fig. 4(b).

3. Feature extraction

Feature extraction is a step to extract the meaningful features from the segmented ROI for later modeling or verification process. In extracting the features, we use the operator-based approach to extract the line-like features of palm-print in the ROI of palm table.

First, we employ the simple Sobel operators to extract the feature points of palm-print. Four-directional Sobel operators S_0, S_{90}, S_{45} , and S_{135} are designed as shown in Fig. 5(a). Consider a pixel of ROI in the palm table, four-directional

Sobel operators are performed to select the maximal value as the resultant value of ROI. This operation is operated according to the following expression:

$$f * S = \max(f * S_0, f * S_{45}, f * S_{90}, f * S_{135}). \quad (1)$$

Here, symbol $*$ is defined as the convolution operation. Sobel's features of ROI are thus obtained as shown in Fig. 5(b).

Next, we present other complex morphological operators to extract the palm-print features. In the gray-scale morphology theory, two basic operations, namely *dilation* and *erosion* for image f are defined as follows:

$$\begin{aligned} \text{Dilation: } (f \oplus b)(s) &= \max\{f(s-x) + b(x) \mid (s-x) \in D_f \\ &\quad \text{and } x \in D_b\}, \end{aligned} \quad (2)$$

$$\begin{aligned} \text{Erosion: } (f \ominus b)(s) &= \min\{f(s+x) - b(x) \mid (s+x) \in D_f \\ &\quad \text{and } x \in D_b\}. \end{aligned} \quad (3)$$

Here, D_f and D_b represent the domains of image f and structuring element b . In addition, two combination operations called *opening* and *closing* are extended for further image processing.

$$\text{Opening: } f \circ b = (f \ominus b) \oplus b, \quad (4)$$

$$\text{Closing: } f \bullet b = (f \oplus b) \ominus b. \quad (5)$$

In Ref. [12], Song and Mevrou designed an edge detector called *alternating sequential filter* (ASF), which provides perfect effects in the noisy or blurry images. The mechanism of ASF is constructed as follows. Two filters are defined as

$$f_1 = \gamma_l \phi_l \quad (6)$$

and

$$f_2 = f_1 \oplus b_{3 \times 3}. \quad (7)$$

The algebraic opening γ_l and closing ϕ_l are defined as

$$\gamma_l = \max(f \circ b_{0,l}, f \circ b_{45,l}, f \circ b_{90,l}, f \circ b_{135,l}) \quad (8)$$

and

$$\phi_l = \min(f \bullet b_{0,l}, f \bullet b_{45,l}, f \bullet b_{90,l}, f \bullet b_{135,l}), \quad (9)$$

where symbols $b_{\alpha,l}$ denote the structuring elements of length l and angle α . In our experiments, value l is set to be 5. Next, the morphological operator is defined to be $f_m = f_2 - f_1$. The edge pixels are thus obtained by using the morphological function $f * f_m$ as shown in Fig. 5(c).

Now, the feature vectors are created in the following way. Consider the training samples, the ROI images are uniformly divided into several small grids. The mean values of pixels in the grids are calculated to obtain the feature values. These values are sequentially arranged row by row to form the feature vectors. In our experiments, three different grid sizes 32×32 , 16×16 and 8×8 are adopted to obtain the multi-resolutional feature vectors.

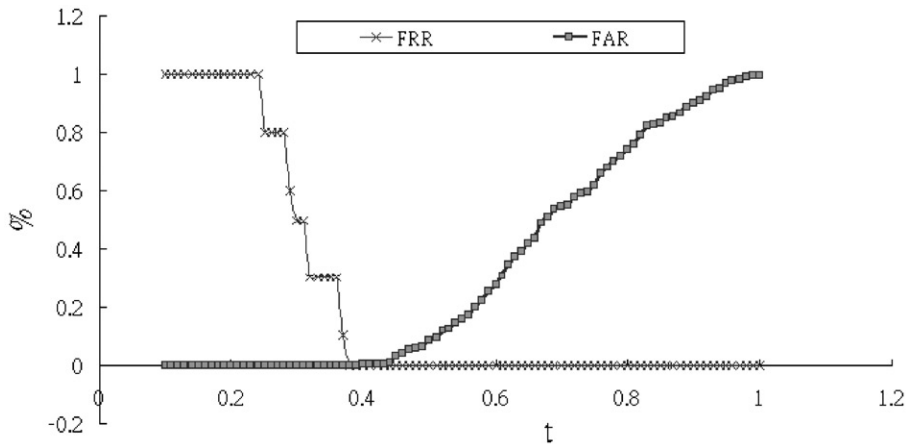


Fig. 6. The FAR and FRR values for a specific individual.

4. Enrollment and verification processes

In a palm-print-based authentication system, two phases, *enrollment* and *verification*, should be executed. In this section, we develop two methods to train the models for these two phases. Firstly, we design a simple and practical technique, *multiple template matching*, to model the verifier of a specific person. Secondly, a *backpropagation* (BP) neural-network-based verifier is constructed. In this approach, the scaled, conjugated gradient technique is applied to find the best weights of BP network in the training process. Lastly, the verification process is introduced by using these two approaches.

4.1. Multi-template-matching approach

Template matching using the correlation function is a common and practical technique utilized in many pattern recognition applications. In this paper, we try to use this approach to perform the verification task to decide whether the query sample is a genuine pattern or not. Consider a query sample x and a template sample y , a *correlation* function is utilized to measure the similarity between the two feature vectors as follows:

$$R_{xy} = \frac{\sum_{i=1}^n (x_i - \mu_x)(y_i - \mu_y)}{\sigma_x \sigma_y}. \quad (10)$$

In Eq. (10), symbols μ and σ represent the mean and standard derivation values, respectively. In addition, value n is the length of feature vectors which is set to be 32×32 , 16×16 , or 8×8 in our experiments. This coefficient value of linear correlation function is calculated for the similarity evaluation.

In creating the reference templates in the enrollment stage, M samples of individual X are collected to form the matching template database. The main advantage of this approach

is that less training time is needed in training the matching model. In the verification stage, the correlation coefficient of query and reference samples is calculated by making use of Eq. (10). If the reference and test patterns are both derived from the same person, then the coefficient value will be approximately one. Otherwise, if the value of similarity approximates to zero, then the query sample should be considered to be a forged pattern.

From the preceding contexts, the metric we define in determining the genuine or forged query sample can be modified to be $1 - R$. Based on this criterion, it is easy to verify the input pattern by a pre-defined threshold value t . If the value $1 - R$ is smaller than threshold t , then the owner of query sample is claimed to be individual X . Otherwise, the query sample is classified as a forged pattern.

In many biometric-based verification models, the selection of threshold value t is the most difficult step in the enrollment stage. It will affect the FAR and false rejection rate FRR (Fig. 6). Basically, these two values contradict each other. The higher the FAR value is, the lower the FRR value becomes, and vice versa. In general, an identification system with lower FAR requirement will be adopted in the higher security system. On the other hand, the systems with lower FRR requirement are used in many user-friendly control systems. The selection of FAR or FRR value depends on the aim of applications. In order to evaluate the verification performance, the sum of FAR and FRR values is defined as the performance index I in this paper. The main goal of threshold selection is to find the minimal values of FAR and FRR for each individual which will depend on the characteristics of samples of individual X . In other words, an individual X should have his own threshold value t_x . The selection process is described in the following paragraph.

First, the *leave-one-out* cross-validation methodology is applied to evaluate the FRR. Consider M template samples

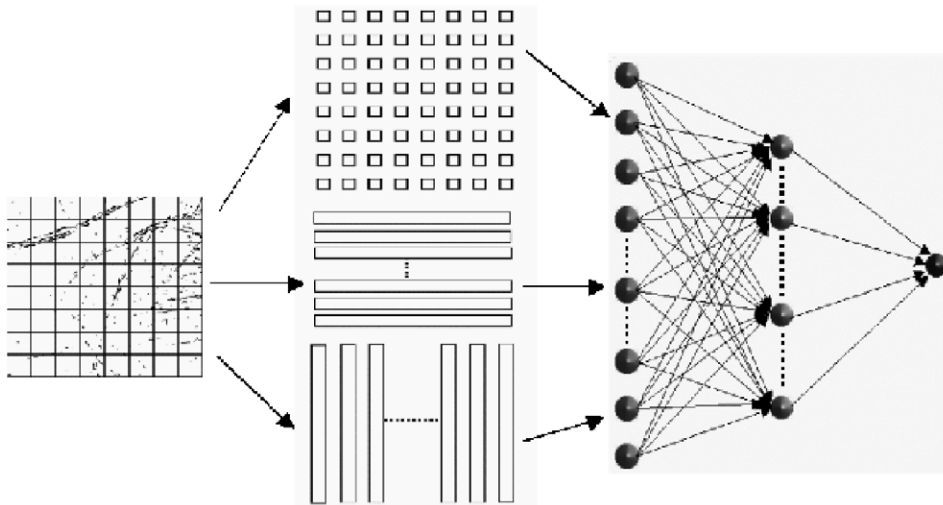


Fig. 7. The mechanism of backpropagation neural network.

of an individual X (called *positive samples*), and N samples of other persons (called *negative samples*). Assume that sample x is a pattern in the M templates. The average distance for sample x to the other $M - 1$ templates is computed to be $d_x = \sum_{j=1}^{M-1} (1 - R_{xj}) / (M - 1)$. Moreover, the distances for the other $M - 1$ reference samples are also obtained. If d_x is larger than the threshold value t_x , then sample x is a forged pattern and the value E_1 (the error number of FRR) should be increased by 1. Similarly, the average distance d_y of a negative sample y to M reference templates is also calculated as $d_y = \sum_{j=1}^M (1 - R_{yj}) / M$. The value E_2 of error number for the computation of FRR is added by 1 when the average distance d_y is smaller than the threshold t_x . The performance index I_x for individual X is thus defined as the summation of FAR plus FRR as follows:

$$I_x = E_1/M + E_2/N. \quad (11)$$

Next, list all the possible threshold values from 0 to 1, and depict the curves of FAR and FRR as shown in Fig. 6. The best value $t_x = 0.38$ with the minimal performance index is chosen to be the threshold value. This threshold value t_x will be used later in a verification process for individual X .

4.2. Backpropagation neural network (BPNN) approach

Backpropagation neural network has been widely utilized in the field of pattern recognition. In this section, we apply this well-known approach to perform the verification task. Similar to the template-matching approach, 64 mean values of windows of size 32×32 in ROI are calculated to obtain the feature vectors. In addition, eight values generated from eight horizontal windows of size 32×256 , and eight values generated from eight vertical windows of size 256×32 are all

calculated to be the 16 elements of feature vectors. These 80 values are input to the BP neural network. The architecture of our proposed network is designed to be a three-layer-based network which includes an input, a hidden and an output layer as depicted in Fig. 7. There are 80, 40 and 1 neurons in each layer, respectively. This similar architecture has also been applied in face detection successfully [13].

The training process of BP neural network includes *sample collection*, *weight initialization*, *forward learning*, and *backward learning* steps. The MATLAB software provides an effective tool to obtain the best weights of BPNN. Now, we focus our attention on the sample collection step. In this step, M image samples of a specific individual X called positive samples and N image samples of other K persons called negative samples are collected to train the BP neural network. In order to increase the verification performance, J artificial generating samples are created from the M positive samples by using the bootstrap algorithm. This algorithm has been applied in generating the sufficient samples in face detection [13]. Consider the ROI of an image sample, we randomly shift it left or right and up or down by 0–5 pixels, and randomly rotate it by -5° to $+5^\circ$. In our experiments, both positive and negative samples are equally created for the simplification of training process. In order to generate the same number of positive and negative samples, JK positive samples are generated by duplicating J positive samples K times for the individual X . On the other hand, JK negative samples are randomly selected from K persons. These $2JK$ samples are input to the network at each training epoch. In addition, the negative samples play a crucial role in determining the threshold values or network. In order to select the samples effectively, the bootstrap methodology [13,14] can be applied to find the precise boundary between the real and forged palm-print samples. The scaled

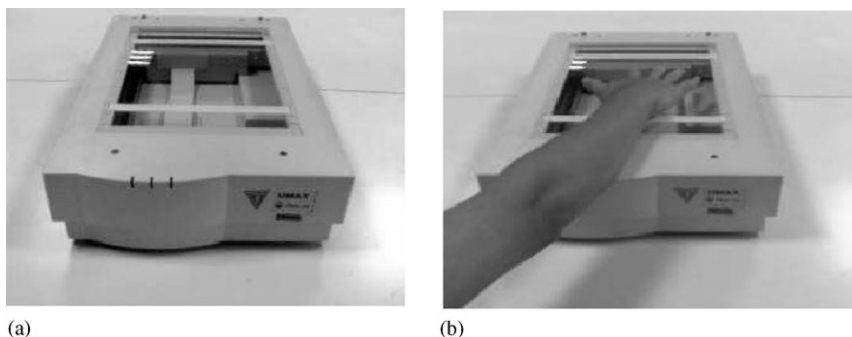


Fig. 8. The input device of palm-print images.

conjugate-gradient algorithm [15] is utilized to adapt the weights with a specified error function in the last three steps.

5. Experimental results

In this section, some experimental results are demonstrated to verify the validity of our approach. First, the experimental environment is set up and described in Section 5.1. Next, the verified results generated by the template matching and BPNN are demonstrated in Sections 5.2 and 5.3, respectively.

5.1. Experimental environment

In our experimental environment, a platform scanner as shown in Fig. 8(a) is used to capture the hand images. Here, the scanner that we use in our system is a color scanner which is a commercial product of UMAX Co. Users are asked to put their right hands on the platform of scanner without any pegs as shown in Fig. 8(b). The hand images of size 845×829 are scanned in gray-scale format and in 100 dpi (dot per inch) resolution. Thirty hand images of each individual are obtained three times within three weeks to construct the database. In the enrollment stage, the first 10 images are used to train the verification model. The other 20 images are tested by the trained verifier. The verification system is programmed by using the C programming language and Matlab developing kits under Microsoft Windows environment. In the following contexts, the experimental results verified by template matching and BP neural network algorithms are reported.

5.2. Verification using template-matching algorithm

In the first experiment, three kinds of window sizes 32×32 , 16×16 , and 8×8 are adopted to evaluate the performance of the template-matching methodology. In each window, the mean value of pixels is computed and considered to be an element of vectors. The linear correlation function is used to calculate the similarity between the reference and test

samples. Consider a person X , 10 samples are chosen to be the reference templates of a verifier. These 10 positive samples of individual X and 490 negative samples of 49 persons are collected to compute the type I and type II errors. The results of FAR and FRR using all the possible threshold values ranging from 0 to 1 for various grid window sizes are calculated to find the best threshold values, respectively. The threshold value t_X for individual X is chosen by the selection rule as stated in the previous section. Thereby, the query samples are verified by the verifier of X and thresholded by the pre-selected value t_X . Two sets of palm-print images are illustrated to denote the matching results as shown in Fig. 9 and Table 1. Furthermore, experiments on 1000 positive samples and $20 \times 50 \times 49$ negative samples of 50 persons are conducted to evaluate the performance. The multiple template-matching algorithm can achieve the accuracy rates above 91% as tabulated in Table 2. In this table, both FAR and FRR values are below 9%.

5.3. Verification using BPNN

In this section, the BPNN architecture is adopted as shown in Fig. 7 to decide whether the query sample is genuine or not. In this experiment, the network for a specific individual X was trained for the latter verification process. Ten positive samples of individual X and 490 negative samples of another 49 persons were all collected to train the BP neural network. In order to obtain the best verification performance, 10 artificially generated samples were generated from each training sample using the bootstrap algorithm. In the training phase, both positive and negative samples were equally created. Four thousand and nine hundred positive samples were generated by duplicating 100 positive samples of individual X 49 times. On the other hand, 4900 negative samples were generated from the hand images of 49 selected persons. These 9800 samples are input to the network at each training epoch. In the testing phase, the other 20 positive images of individual X are verified by the trained BP neural network to evaluate the FRR value. Besides, 20×49 negative samples are also tested to compute the FAR value. In this experiment, 50 persons were selected and tested by

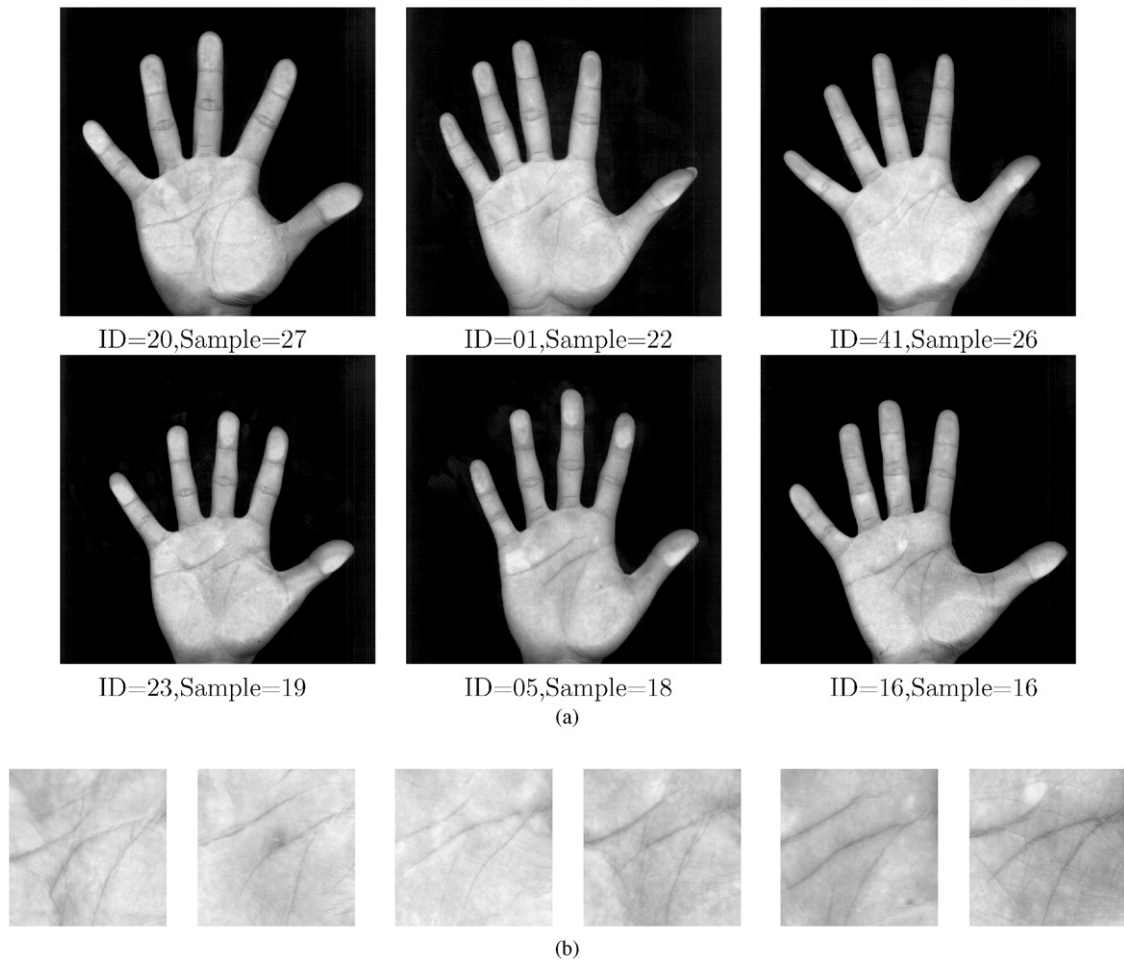


Fig. 9. The illustrated palm-print samples: (a) the original images; (b) and their corresponding ROI images.

Table 1
Two illustrated examples using the template matching and the BP neural network

Feature	Sobel features				Morphological features			
	S8 × 8	S16 × 16	S32 × 32	BPNN	M8 × 8	M16 × 16	M32 × 32	BPNN
<i>A successful case, and the testing ID = 20</i>								
T_{20}	0.510	0.620	0.680	0.650	0.550	0.640	0.730	0.750
ID = 20, $S = 27$	0.152	0.215	0.317	0.311	0.193	0.239	0.353	0.296
ID = 1, $S = 22$	0.799	0.853	0.904	0.915	0.945	0.888	0.941	0.913
ID = 41, $S = 26$	0.706	0.789	0.811	0.878	0.699	0.829	0.919	0.877
<i>A failed case, and the testing ID = 23</i>								
T_{23}	0.300	0.390	0.480	0.490	0.340	0.450	0.550	0.520
ID = 23, $S = 19$	0.313	0.412	0.567	0.514	0.363	0.474	0.657	0.613
ID = 5, $S = 18$	0.272	0.382	0.470	0.472	0.339	0.430	0.538	0.478
ID = 16, $S = 16$	0.295	0.385	0.445	0.423	0.323	0.437	0.524	0.481

Table 2
Experimental results using template matching and the BP neural network

Feature	Sobel features				Morphological features			
	S8 × 8	S16 × 16	S32 × 32	BPNN	M8 × 8	M16 × 16	M32 × 32	BPNN
FRR	7.8%	4.5%	4.9%	0.6%	5.5%	3.3%	5.2%	0.5%
FAR	5.9%	6.7%	6.4%	1.79%	6.2%	6.6%	8.7%	0.96%

their corresponding neural networks. The experimental results are listed in Table 2, and the average accuracy rates are both above 98% for Sobel's and morphological features. Besides, both FAR and FRR values are below 2%.

6. Conclusions

In this paper, a novel approach is presented to authenticate individuals by using their palm-print features. The hand images are captured from a scanner without any fixed peg. This mechanism is very suitable and comfortable for all users. Besides, we propose two verification mechanisms, one is the template-matching method and the other is neural network-based method, to verify the palm-print images. In the template-matching method, the linear correlation function is adopted as the metric measurement. Using this method, we can achieve above 91% accuracy rate. In the neural network-based method, we use the backpropagation mechanism and the scaled conjugate-gradient algorithm to build-up a neural-network-based verifier. Using this verifier, we can obtain above 98% accuracy rate. Experimental results reveal that our proposed approach is feasible and effective in personal authentication using palm-print features.

7. Summary

Recently, biometric features have been widely used in many personal authentication applications. Biometrics-based authentication is a verification approach using the biological features inherent in each individual. They are processed based on the identical, portable, and arduous duplicate characteristics. Thus, many access control systems adopt biometric features to replace the digit-based password. In this paper, we propose a scanner-based personal authentication system using the palm-print features. It is very suitable in many network-based applications.

The authentication system consists of enrollment and verification stages. In the enrollment stage, M hand images of an individual are collected as the training samples. These samples should be processed by the *pre-processing*, *feature extraction*, and *modeling* modules to generate the matching templates. In the verification stage, a query sample is also processed by the pre-processing and feature extraction modules, and is then matched with the templates to decide

whether it is a genuine sample or not. In our proposed palm-print-based identification system, the pre-processing module, including *image-thresholding*, *border-tracing*, *wavelet-based segmentation*, and *ROI location* steps, should be performed to obtain a square region in a palm table which is called ROI. Then, we perform the feature extraction process to obtain the feature vectors by the Sobel and morphological operations. The reference templates for a specific user are generated in the modeling module. In the verification stage, we use template matching and BPNN to measure the similarity between the reference templates and test samples.

In our experiments, the samples are verified by the template-matching and BP neural-network algorithms. In the first experiment, three kinds of window sizes 32×32 , 16×16 , and 8×8 are adopted to evaluate the performance of the template-matching methodology. The multiple template-matching algorithm can achieve the accuracy rates above 91%. Both FAR and FRR values are below 9%. Next, the BPNN architecture is adopted to decide whether the query sample is a genuine or not. In this experiment, the average accuracy rates are above 98% for both Sobel's and morphological features. Besides, both FAR and FRR values are below 2%. Experimental results verify the validity of our proposed approaches in personal authentication.

References

- [1] R. Clarke, Human identification in information systems: Management challenges and public policy issues, *Inf. Technol. People* 7 (4) (1994) 6–37.
- [2] A.K. Jain, R. Bolle, S. Pankanti, *Biometrics: Personal Identification in Networked Society*, Kluwer Academic Publishers, Dordrecht, 1999.
- [3] L. O'Gorman, Fingerprint verification, in: A.K. Jain, R. Bolle, S. Paukauti (Eds.), *Biometrics: Personal Identification in Networked Society*, Kluwer Academic Publishers, Dordrecht, 1999, pp. 43–64 (Chapter 2).
- [4] M. Golfarelli, D. Miao, D. Maltoni, On the error-reject trade-off in biometric verification systems, *IEEE Trans. Pattern Anal. Mach. Intell.* 19 (7) (1997) 786–796.
- [5] R.L. Zunkei, Hand geometry based verification, in: A.K. Jain, R. Bolle, S. Pankanti (Eds.), *Biometrics: Personal Identification in Networks Society*, Kluwer Academic Publishers, Dordrecht, 1999, pp. 87–101 (Chapter 4).

- [6] A.K. Jain, N. Duta, Deformable matching of hand shapes for verification, <http://www.cse.msu.edu/~dutanico/>, 1999.
- [7] D. Zhang, W. Shu, Two novel characteristics in palm-print verification: datum point invariance and line feature matching. *Pattern Recognition* 32 (1999) 691–702.
- [8] S.Y. Kung, S.H. Lin, M. Fang, A neural network approach to face/palm recognition, in: *Proceedings of the International Conference on Neural Networks*, 1995, pp. 323–332.
- [9] D.G. Joshi, Y.V. Rao, S. Kar, V. Kumar, R. Kumar, Computer-vision-based approach to personal identification using finger crease pattern, *Pattern Recognition* 31 (1) (1998) 15–22.
- [10] D.D. Zhang, *Automated Biometrics: Technologies and Systems*, Kluwer Academic Publishers, Dordrecht, 2000.
- [11] M. Sonka, V. Hlavac, R. Boyle, *Image Processing, Analysis, and Machine Vision*, PWS Publisher, 1999.
- [12] X. Song, C.W. Lee, S. Tsuji, Extraction facial features with partial feature template, in: *Proceedings of the Asian Conference on Computer Vision*, 1993, pp. 751–754.
- [13] H.A. Rowley, S. Baluja, T. Kanade, Neural network-based face detection, *IEEE Trans. Pattern Anal. Mach. Intell.* 20 (1) (1998) 23–38.
- [14] K.K. Sung, *Learning and example selection for object and pattern detection*, Ph.D. Thesis, MIT, Cambridge, MA, anonymous ftp from publications.ai.mit.edu, 1996.
- [15] M.F. Moller, A scaled conjugate gradient algorithm for fast supervised learning, *Neural Network* 6 (1993) 525–533.

About the Author—CHIN-CHUAN HAN received the B.S. degree in Computer Engineering from National Chiao-Tung University in 1989, and an M.S. and a Ph.D. degree in Computer Science and Electronic Engineering from National Central University in 1991 and 1994, respectively. From 1995 to 1998, he was a Postdoctoral Fellow in the Institute of Information Science, Academia Sinica, Taipei, Taiwan. He was an Assistant Research Fellow in the Applied Research Lab., Telecommunication Laboratories, Chunghwa Telecom Co. in 1999. He is currently an Assistant Professor in the Department of Computer Science and Information Engineering, Chunghua University. His research interests are in the areas of face recognition, biometrics authentication, image analysis, computer vision, and pattern recognition.

About the Author—HSU-LIANG CHENG received his B.S. degree from the Department of Mathematics, Chung Yuan Christian University, Taiwan, in 1997, and his M.S. degree in computer science and information engineering from National Central University, Taiwan, in 2000. His current interests include pattern recognition, biometrics authentication, and machine learning.

About the Author—CHIH-LUNG LIN is working towards his Ph.D. in Computer Science and Electronic Engineering at National Central University since 1999. His research interests include biometrics authentication, pattern recognition, and image processing.

About the Author—KUO-CHIN FAN was born in Hsinchu, Taiwan, on 21 June 1959. He received his B.S. degree in Electrical Engineering from National Tsing-Hua University, Taiwan, in 1981. In 1983, he worked for the Electronic Research and Service Organization (ERSO), Taiwan, as a Computer Engineer. He received his graduate degree in Electrical Engineering at the University of Florida in 1984 and received the M.S. and Ph.D. degrees in 1985 and 1989, respectively. From 1984 to 1989 he was a Research Assistant in the Center for Information Research at University of Florida. In 1989, he joined the Institute of Computer Science and Information Engineering at National Central University where he became a professor in 1994. From 1994 to 1997 he was chairman of the department. Currently, he is the director of the Computer Center. He is a member of IEEE and SPIE. His current research interests include image analysis, optical character recognition, and document analysis.